Macromolecular Research

Article

DOI 10.1007/s13233-019-7145-x

www.springer.com/13233 pISSN 1598-5032 eISSN 2092-7673

Synthesis and Functionalization of Ynone-Based Tubular Microporous Polymer Networks and Their Carbonized Products for CO_2 Capture

Jeongmin Lee
Ji Young Chang*

Department of Materials Science and Engineering, College of Engineering, Seoul National University, Seoul 08826, Korea

Received December 16, 2018 / Revised March 20, 2019 / Accepted March 23, 2019

Abstract: Ynone-based microporous polymer networks (YMPNs) were synthesized by the reaction of aromatic dicarboxylic acid chloride and alkyne groups under Sonogashira cross-coupling reaction conditions. As the reaction proceeded in a mixture of toluene and triethylamine (TEA), tubular precipitates formed rapidly. The microscopic and XRD studies showed that the precipitates had a core-shell structure with a rod-shaped triethylammonium chloride (TEA-HCl) crystalline core and a polymeric shell. The core was removed by washing with methanol to provide a hollow polymeric tube. The TEA-HCl rod formed *in situ* during the cross-coupling reaction and served as a template in forming the tubular morphology. YMPNs could be modified with ease because of the presence of highly reactive ynone groups. YMPNs were functionalized with ethylenediamine by the Michael-type addition reaction. The amino group functionalized YMPNs were used as precursors of nitrogen-doped porous carbons. The pyrolysis of the polymers at 800 °C produced microporous carbon materials without the activation process. The carbon materials showed significantly enhanced Brunauer-Emmett-Teller (BET) surface areas and CO_2 uptake capacities compared to their precursor polymers.

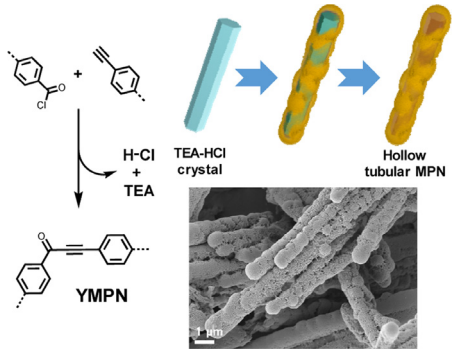

Keywords: microporous polymer network, ynone, pyrolysis, porous carbon, CO_2 adsorption.

1. Introduction

Microporous polymer networks (MPNs) have attracted significant attention due to their potential applications including gas separation and storage,[1,2] heterogeneous catalysis,[3-5] photoluminescence,[6,7] and removal of pollutants.[8,9] MPNs have an advantage of flexibility in structural design compared with carbon and inorganic microporous materials. The majority of MPNs are synthesized by the polymerization of multifunctional monomers to have highly cross-linked network structures. A wide range of monomers and various polymerization methods have been used to synthesize MPNs with diverse chemical structures. MPNs with functional groups generated during the polymerization are of particular interest because their pore structures and surface properties can be further adjusted by post-reactions.

Ynones are α,β-unsaturated ketones, which are highly reactive due to the presence of polarized C-C triple bonds and carbonyl groups. Ynones serve as Michael acceptors and react with amines and alcohols to produce aminoenones[10] and alkoxyenones,[11] respectively. Ynones are synthesized by the reaction of a metal acetylide with a carbonyl compound, the oxidation of an alkyne, and a metal catalyzed cross-coupling reaction of terminal alkyne and aryl or vinyl halide groups in the presence of carbon monoxide.[12] Ynones can also be obtained by the reaction between acyl halide and alkyne groups under Sonogashira cross-coupling conditions. Recently, the coupling methods of synthesizing ynones have been employed for the preparation of functional conjugated polymers. For example, Tang *et al.* prepared amino and thiol group functionalized conjugated polymers by the tandem polymerization of a diyne and a dicarbonyl dichloride in the presence of an amine and a thiol, respectively.[13-16] Son *et al.* synthesized an ynone group-containing MPN by the coupling reaction of alkyne and aryl halide groups under a carbon monoxide atmosphere.[17,18]

In this work, we synthesized ynone-based MPNs with tubular morphology by the reaction of acyl chlorides and alkyne monomers under Sonogashira cross-coupling conditions. The MPNs were functionalized with amino groups by the Michael-type addition reaction and then pyrolyzed to produce N-rich microporous carbons. The carbonization of MPNs could be an interesting way to produce microporous carbons without any activation processes. Chemical properties of microporous carbons such as polarity and basicity might be tuned by *in situ* heteroatom doping using heteroatom containing MPN precursors.[19-21] Microporous materials are promising adsorbents for the capture of CO_2, which is the main greenhouse gas responsible for global warming.[22,23] We studied pore structures and CO_2 adsorption capacities of the MPNs and their carbonized materials.

2. Experimental

2.1. Materials

1,3,5-Triethynylbenzene, 1,4-diethynylbenzene, 1,3,5-benzen-

Acknowledgments: This research was supported by the National Research Foundation of Korea (NRF) grant funded by the Korea government (MSIP) (No. 2015R1A2A2A01006585).

***Corresponding Author:** Ji Young Chang (jichang@snu.ac.kr)

etricarbonyl trichloride, terephthaloyl chloride, and bis(triphenylphosphine)palladium(II) dichloride were purchased from Tokyo Chemical Industry. Copper iodide and ethylenediamine anhydrous were purchased from Sigma-Aldrich. Toluene and triethylamine (TEA) were purchased from Alfa Aesar. All chemicals were used without further purification.

2.2. Instrumental characterization

Scanning electron microscopy (SEM) study was conducted using a JEOL JSM-6330F microscope. Transmission electron microscope (TEM) images were obtained by a JEOL JEM-2010 microscope at 200 keV. TEM samples were dispersed in ethanol and dropped onto a TEM grid. Solid state ^{13}C nuclear magnetic resonance spectra were measured on a Bruker Avance II NMR spectrometer (125 MHz) using a cross polarization total sideband suppression (CP/TOSS) technique. Fourier transform infrared (FT-IR) absorption spectra were recorded with a Bruker VERTEX80v spectrometer using KBr pellets. Powder X-ray diffraction (XRD) data were collected on a Bruker New D9 Advance diffractometer using a CuKα beam source (λ=1.5418 Å). Surface areas were measured with a Belsorp-Max (BEL Japan Inc.) apparatus with ultra-high purity nitrogen gas (99.999%) at 77 K. Samples were degassed at 80 °C for 12 h under vacuum before analysis. The pore size distribution diagrams were calculated from the isotherms using the nonlocal density functional theory (NL-DFT). CO_2 isotherms were measured at 273 K on a Belsorp-Max (BEL Japan Inc.). The selectivity of CO_2/N_2 was obtained by an initial slope calculation method from gas adsorption data at a low pressure range (0-0.15 bar). Thermogravimetric analysis (TGA) was performed on a TA modulated TGA2050 with a heating rate of 10 °C/min under nitrogen.

2.3. Synthesis of ynone based microporous polymer networks (YMPN-1 and YMPN-2)

YMPN-1 and YMPN-2 were synthesized by the reaction of acyl chlorides and arylacetylenes under Sonogashira cross-coupling reaction conditions. For YMPN-1, 1,3,5-triethynylbenzene (100 mg, 0.67 mmol) and terephthaloyl chloride (135.2 mg, 0.67 mmol) were added to a mixture of $PdCl_2(PPh_3)_2$ (21 mg, 0.03 mmol), CuI (5.5 mg, 0.03 mmol), toluene (12 mL), and triethylamine (0.4 mL) at room temperature. The mixture was heated to 60 °C and was stirred at the same temperature for 12 h under nitrogen atmosphere. The solution turned to brownish color within 30 min. After the reaction finished, the insoluble precipitates were filtered and successively washed with methanol, acetone, and THF. The polymer was further purified by Soxhlet extraction with methanol and THF for 12 h each and dried *in vacuo* to give a light brownish powder (yield: 175 mg, 94.1%). The same procedure was used in the synthesis of YMPN-2, using 1,4-diethynylbenzene (126.2 mg, 1 mmol) and 1,3,5-Benzenetricarbonyl trichloride (177 mg, 0.67 mmol) as monomers (yield: 220 mg, 95.5%).

2.4. Functionalization of YMPNs with ethylenediamine

In a typical procedure, YMPN-1 (100 mg) was dispersed in methanol (20 mL) by sonication. After the addition of an excess amount of ethylenediamine (0.3 mL), the suspension was refluxed for 12 h under nitrogen atmosphere. The insoluble polymer was filtered, purified by Soxhlet extraction with methanol for 12 h, and dried *in vacuo* to give YMPN-1-N. The same procedure was used in the synthesis of YMPN-2-N, using YMPN-2 instead of YMPN-1.

2.5. Carbonization of YMPNs

A precursor polymer (150 mg) in an alumina boat was placed in a tube furnace. After purging with nitrogen gas at RT for 1 h, the tube furnace was heated to 800 °C with a heating rate of 5 °C min^{-1}. Carbonization was conducted at 800 °C for 2 h under nitrogen.

3. Results and discussion

The Sonogashira cross-coupling reaction of aryl halide and

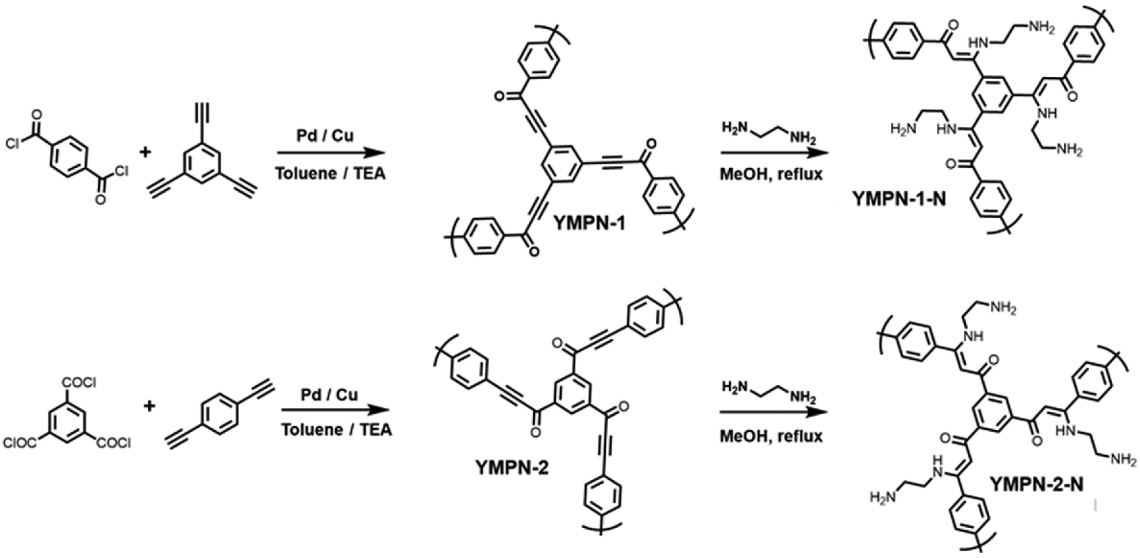

Figure 1. Synthesis of YMPNs and their amine-functionalized derivaties.

alkyne groups has been widely used for the synthesis of MPNs with conjugated structures,[24] but the cross-coupling reaction between carboxylic acid chloride and alkyne groups has been little studied in the MPN synthesis. The Pd catalyzed reaction between acid chloride and alkyne groups is considered as a rapid and high-yielding method for the synthesis of ynones.[12,25] For example, Cox *et al*. reported that the reaction between phenylacetylene and benzoyl chloride with a Pd catalyst and CuI was completed within 10 min to produce an ynone.[25] We prepared an ynone based microporous polymer networks, YMPN-1 by the coupling reaction of an aromatic dicarboxylic acid dichloride and 1,3,5-triethynylbenzene in a mixture of toluene and TEA in the presence of $PdCl_2(PPh_3)_2$ and CuI (Figure 1). As the reaction proceeded, the reaction mixture turned to brown color and precipitates formed rapidly. YMPN-1 was obtained as light brownish powders in nearly quantitative yield after filtration and washing with organic solvents. YMPN-2 was prepared from an aromatic tricarboxylic acid trichloride with 1,4-diethynylbenzene in the same manner.

YMPN-1 and YMPN-2 had alkyne units conjugated to carbonyl groups. The alkyne groups were polarized and thus were susceptible to the nucleophilic attack by various nucleophiles such as amines. We introduced amino functionality to YMPN-1 and YMPN-2 by the reaction with ethylenediamine to give YMPN-1-N and YMPN-2-N, respectively. The reaction of an ynone with a primary amine was previously reported to show excellent stereo-selectivity and high efficiency.[10]

Microstructures of YMPN-1 and YMPN-2 were studied by SEM and TEM (Figure 2). The TEM images (Figure 2(c) and 2(f)) revealed that both YMPN-1 and YMPN-2 possessed hollow tubular structures. The inner diameters of tubes were a few hundred nanometers, and the lengths of the tubes were in the range of a few tens micrometers. The tubes of YMPN-2 showed more smooth surfaces than those of YMPN-1. The tubular structures of the polymers did not change significantly even after the functionalization with ethylenediamine (Figure S1). Considering the cross-linked nature of the polymers, their tubular morphologies were intriguing. Shape controlled microporous polymers such as microporous capsules have been generally synthesized using a template method.[26-28] A few examples of tubular cross-linked polymers obtained by the Sonogashira cross-coupling reaction of aryl halide and alkyne groups without any external templates were reported,[29-31] but their formation mechanisms were not fully understood.

We analyzed the precipitates after a reaction time of 30 min to study the mechanism of the tubular structure formation. The SEM images of the early products showed rods covered with small particles (Figure 3(a)). The XRD pattern (Figure 3(b)) suggested that the core rods were crystalline TEA-HCl. In the cross-coupling reaction between a carboxylic chloride and a terminal alkyne in a mixture of toluene and TEA, HCl would be released and react with TEA to form a TEA-HCl salt. We presumed that the insoluble TEA-HCl salt was crystallized into a rod shape and served as a template in the formation of the tubular morphology. Insoluble polymer particles would adhere to the surface of the TEA-HCl rod to reduce the total surface energy, and the coupling reaction continued to take place on the rod surface. After the completion of the reaction, the core TEA-HCl rod was removed by washing with methanol to yield a hollow tubular polymer structure. Recently, we observed similar results in the Pd-alkyne dehydrohalogenation reaction, where an *in situ* formed TEA-HCl rod acted as a template to produce a tubular structure.[32] The possible mechanism of the tubular structure formation is schematically drawn in Figure 3(c).

The chemical structures of YMPN-1 and YMPN-2 were confirmed by FT-IR and solid state ^{13}C CP/TOSS NMR spectroscopy (Figure 4(a), (b)). In the FT-IR spectra, both polymers showed the characteristic peak of the polarized alkyne at 2200 cm^{-1}. The strong peak at 1650 cm^{-1} was assigned to carbonyl groups. After the reaction with ethylenediamine, the intensity of the alkyne peak significantly decreased, indicating the conversion of alkyne groups to alkene groups.[16] The carbonyl peak was shifted

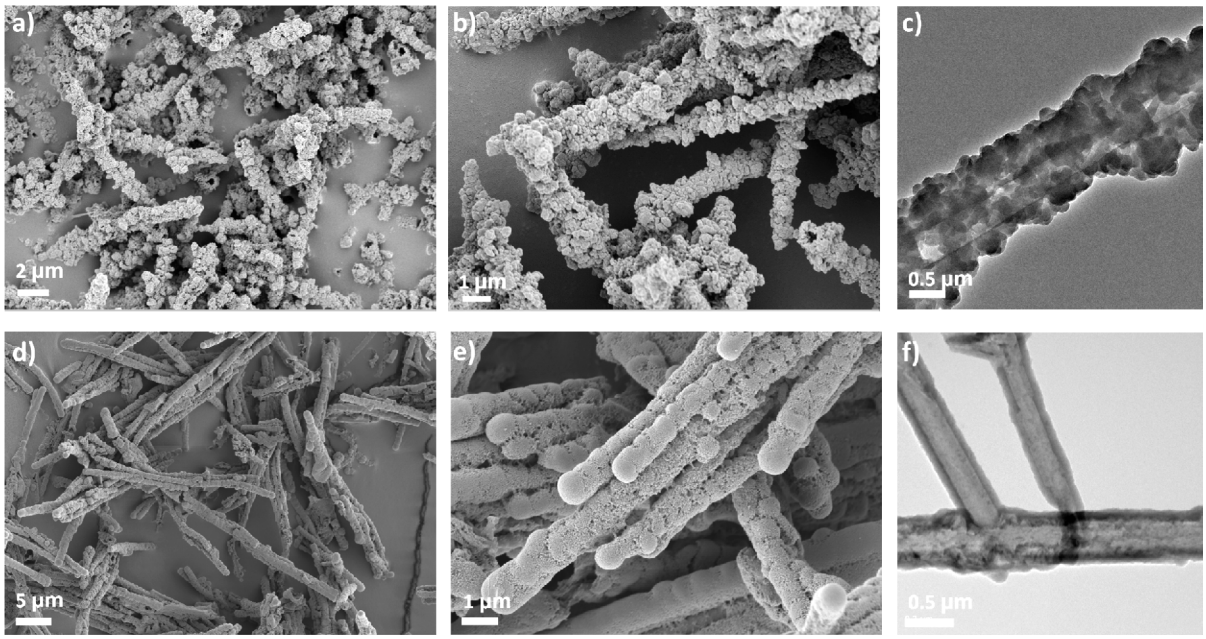

Figure 2. SEM and TEM images of YMPN-1 (a-c) and YMPN-2 (d-f).

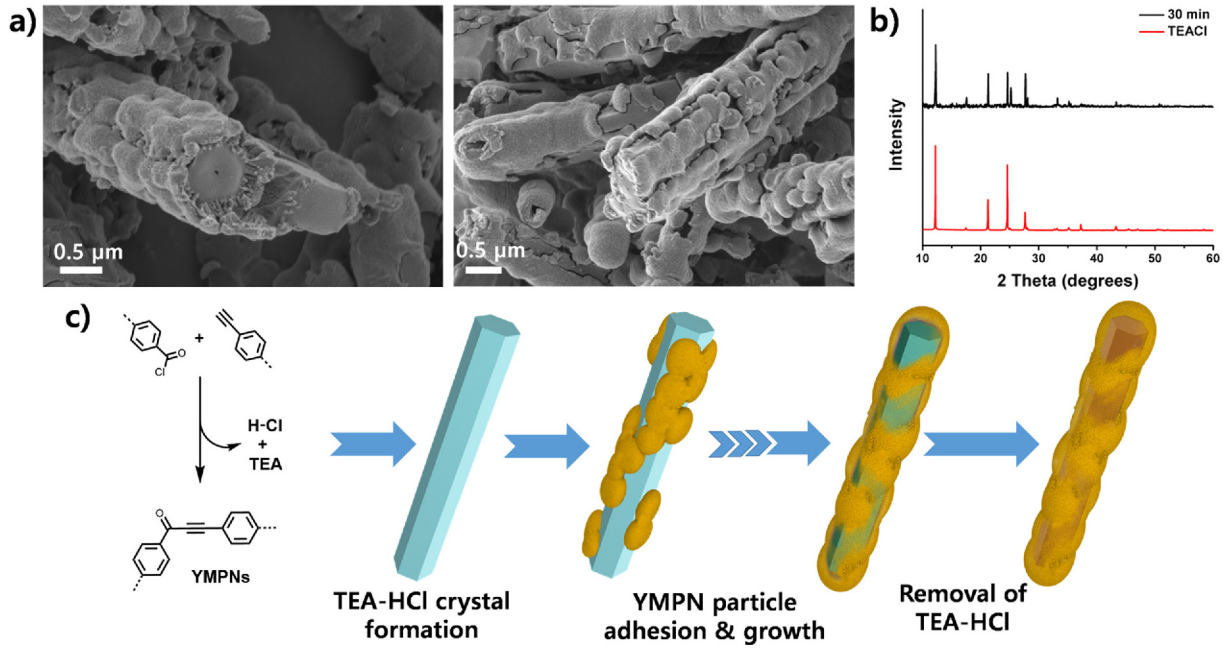

Figure 3. (a) SEM images and (b) XRD patterns of the precipitates after a reaction time of 30 min. (c) Schematic illustration of the formation mechanism of a tubular microstructure.

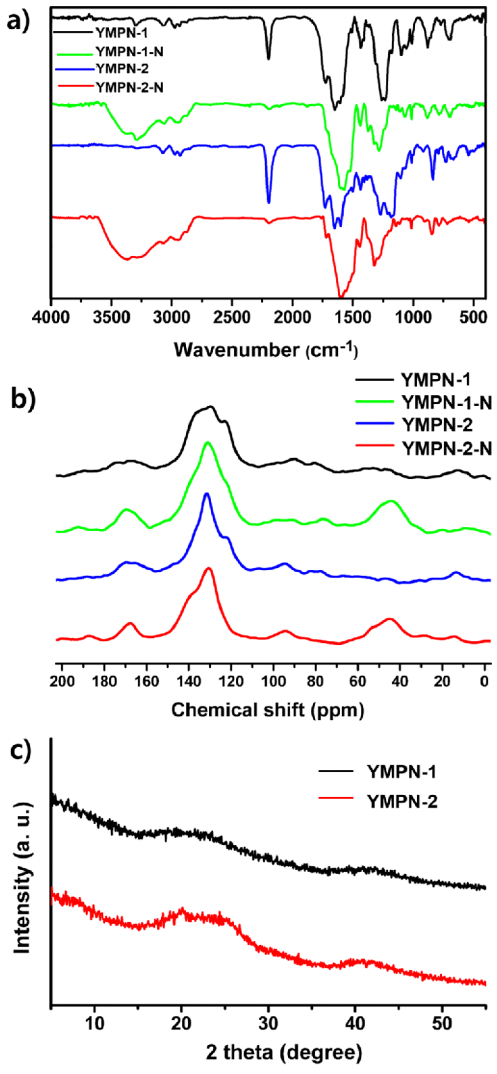

Figure 4. (a) FT-IR and (b) solid-state ^{13}C NMR spectra of YMPNs. (c) XRD patterns of YMPN-1 and YMPN-2.

to 1600 cm^{-1} and overlapped with the N-H bending peak at 1615 cm^{-1}.[33] The solid state ^{13}C NMR spectra of the polymers showed the peaks at 137, 131, and 122 ppm, corresponding to the aromatic carbons adjacent to the carbonyl carbon, hydrogen, and acetylene carbon, respectively. The peak at around 171 ppm was assigned to carbonyl carbons. The internal alkyne carbon peaks appeared at around 92 ppm. The peaks at 78 ppm corresponded to diacetylene carbons, indicating that the homo coupling reaction between ethynyl groups occurred.[34] After functionalization with ethylenediamine, a new broad aliphatic carbon peak centered at 44 ppm appeared. The carbonyl carbon peak was downfield shifted to near 190 ppm and the newly formed alkene carbon peaks appeared at 168 (N-C=) and 94 (H-C=) ppm.[13] The XRD patterns of the polymers measured after washing with organic solvents showed no distinct peaks, indicating the amorphous nature of the polymers as well as the removal of the crystalline TEA-HCl (Figure 4(c)). The TGA thermograms showed that YMPNs were thermally stable up to 250 °C. After the introduction of ethylenediamine groups, a weight loss of 2~5% was observed at 200 °C (Figure S2).

The pore structures of YMPNs were investigated by the nitrogen gas adsorption-desorption isotherm measurements at 77 K (Figure 5(a), Table S1). A steep increase of nitrogen uptake at the low relative pressure region (P/P_0<0.01) was observed in both polymers, indicating the presence of abundant micropores. The pore size distributions of YMPN-1 and YMPN-2, determined based on NL-DFT, also showed the presence of micro- and mesopores (Figure 5(b)). The Brunauer-Emmett-Teller (BET) surface areas of YMPN-1 and YMPN-2 were 498 and 166 m^2 g^{-1}, and the total pore volumes were 0.35 and 0.23 cm^3 g^{-1}, respectively. After functionalization with ethylenediamine, the BET surface areas and total pore volumes of YMPN-1-N and YMPN-2-N decreased to 236 and 81 m^2 g^{-1} and 0.19 and 0.14 cm^3 g^{-1}, respectively (Table S1), possibly due to pore filling by the amino

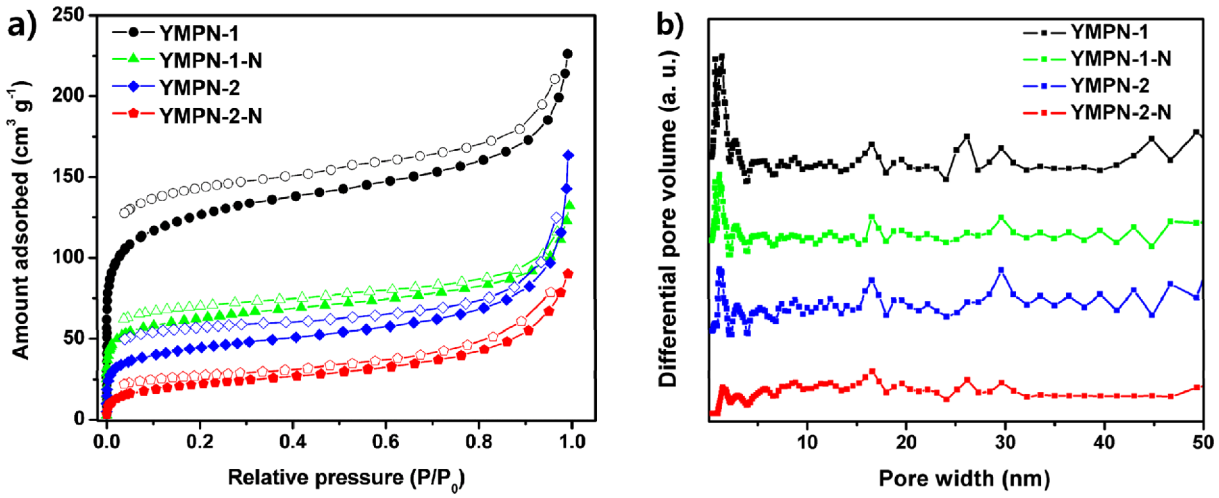

Figure 5. (a) Nitrogen adsorption (filled symbols)-desorption (open symbols) isotherms of YMPNs measured at 77 K and (b) pore size distributions calculated by NL-DFT.

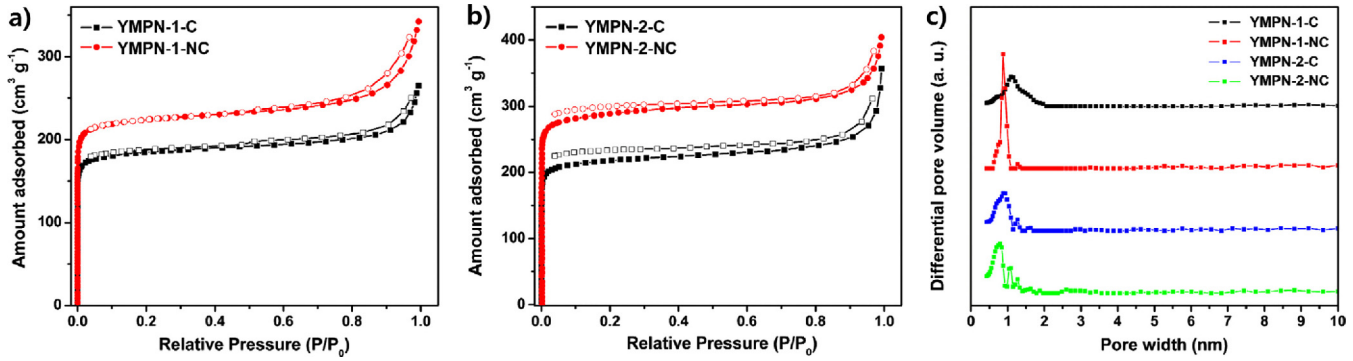

Figure 6. (a, b) Nitrogen adsorption (filled symbols)-desorption (open symbols) isotherms measured at 77 K and (c) pore size distributions of the carbon materials derived from YMPNs.

groups.[35]

Various organic materials have been used as precursors of porous carbon materials. The pyrolysis of organic precursors usually produces carbon materials with relatively low surface areas. The microporosity and high surface areas of porous carbon materials are created by subsequent physical or chemical activation.[36] Since YMPNs had rigid and microporous structures, their pyrolysis was expected to produce microporous carbons without any activation processes. Amino group-functionalized microporous polymers, YMPN-1-N and YMPN-2-N, were carbonized at 800 °C to yield nitrogen doped microporous carbon materials, YMPN-1-NC and YMNP-2-NC, respectively. The tubular morphologies of YMPNs were preserved even after the pyrolysis (Figure S1). The nitrogen contents of YMPN-1-NC and YMPN-2-NC measured by elemental analysis were 3.52 and 3.77 wt%, respectively. Their precursor polymers, YMPN-1-N and YMPN-2-N, showed 9.38 and 10.34 wt% of nitrogen contents, respectively.

Compared with the precursor polymers (YMPN-1-N and YMPN-2-N), YMPN-1-NC and YMPN-2-NC showed much enhanced BET surface areas of 902 and 1158 m^2 g^{-1} and total pore volumes of 0.5 and 0.61 cm^3 g^{-1}, respectively (Figure 6). The carbon materials, YMPN-1-C and YMPN-2-C, obtained from YMPN-1 and YMPN-2, respectively, under the same conditions also exhibited higher BET surface areas and total pore volumes than their precursor polymers. However, these values were significantly lower than those of YMPN-1-NC and YMPN-2-NC, suggesting that the introduced ethylenediamine groups acted as an activation agent during the carbonization process to increase the surface areas.[37]

The capture and sequestration of CO_2 by porous materials have been heavily researched because CO_2 is one of the major greenhouse gases responsible for global warming.[38-40] To improve CO_2 adsorption capacity, the surfaces of porous materials are often modified by grafting with polar functional groups having good affinity with CO_2 molecules. The CO_2 adsorption behaviors of the polymers were measured at 273 K (Figure 7 and Table 1). YMPN-1 and YMPN-2 had a relatively low CO_2 adsorption capacity. After the modification with amino groups, their CO_2 adsorption capacities increased even though the BET surfaces decreased (Figure S3). YMPN-1-C and YMPN-2-C showed higher CO_2 uptake capacities (89.0 and 100.8 cm^3 g^{-1}, respectively) than their precursors. Among the measured samples, the nitrogen doped carbon, YMPN-2-NC exhibited the highest CO_2 adsorption capacity (137.8 cm^3 g^{-1} at 273 K), followed by YMPN-1-NC (101.2 cm^3 g^{-1} at 273 K). The initial CO_2 adsorption slope became steeper after the amino group functionalization. Since the surface properties of the materials would greatly influence the CO_2 adsorption at low pressures, we presumed that the introduced N atoms enhanced the interaction between the framework and CO_2 molecules (Figure S4).[41] The selectivity of CO_2 over N_2 was determined based on the initial uptake slopes of the materials. YMPN-2-NC

Table 1. Porosity and CO_2 uptake data of the carbonized materials

	SA_{BET}[a] (m^2 g^{-1})	V_{total}[b] (cm^3 g^{-1})	V_{micro}[c] (cm^3 g^{-1})	Average pore size (nm)	CO_2 uptake[d] (cm^3 g^{-1})	Selectivity[e] (CO_2/N_2)
YMPN-1-C	743	0.41	0.28	2.16	89.0	29.6
YMPN-1-NC	902	0.50	0.34	2.30	101.2	32.1
YMPN-2-C	874	0.51	0.33	2.39	100.8	21.7
YMPN-2-NC	1158	0.61	0.49	2.13	137.8	41.0

[a]Calculated using the BET method. [b]V_{total} = pore volume at P/P_0 = 0.99. [c]V_{micro} = pore volume at P/P_0 = 0.1. [d]Measured at 273 K. [e]Calculated by the initial slope calculation method.

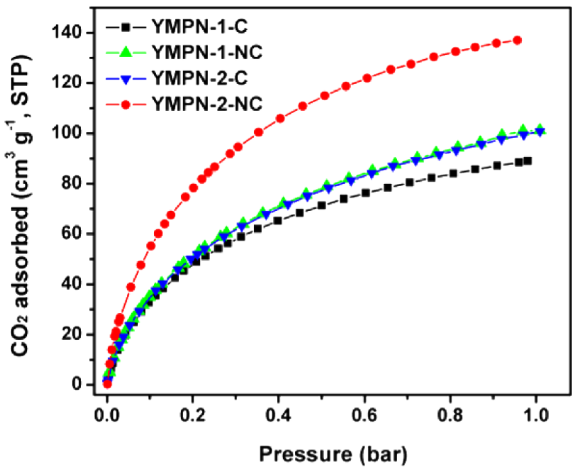

Figure 7. CO_2 adsorption isotherms of YMPN-1-C, YMPN-1-NC, YMPN-2-C, and YMPN-2-NC measured at 273 K.

exhibited the highest selectivity of 41. The excellent CO_2 adsorption properties of YMPN-2-NC could be attributable to its high micropore volume as well as the nitrogen doping effect.

4. Conclusions

In summary, we synthesized ynone-based tubular microporous polymer networks by the coupling reaction between acyl chloride and terminal alkyne monomers. The tubular structures were constructed by the template guided process, where *in situ* formed TEA-HCl rods acted as a template. Using ynone groups as a Michael acceptor, ethylenediamine was grafted to the polymer frameworks. The amino group functionalized MPNs were used as precursors of N-doped porous carbons, which showed high CO_2 adsorption capacities. Since ynone based microporous polymers could be easily modified by the reaction with various functional nucleophiles, they would find wide uses in gas adsorption, separation, and catalysis.

Supporting Information: Information is available regarding the characterization data of the polymers and carbonized materials including the SEM images, TGA thermograms, and CO_2 adsorption test results. These materials are available *via* the Internet at http://www.springer.com/13233.

References

(1) R. Dawson, D. J. Adams, and A. I. Cooper, *Chem. Sci.*, **2**, 1173 (2011).
(2) S. Kim and Y. M. Lee, *Prog. Polym. Sci.*, **43**, 1 (2015).
(3) Y. Xie, T. T. Wang, X. H. Liu, K. Zou and W. Q. Deng, *Nat. Commun.*, **4**, 1960 (2013).
(4) Z.-D. Ding, W. Zhu, T. Li, R. Shen, Y. Li, Z. Li, X. Ren and Z.-G. Gu, *Dalt. Trans.*, **46**, 11372 (2017).
(5) J. G. Kim, J. Lee, J. Lee, S. I. Jo, and J. Y. Chang, *Macromol. Res.*, **25**, 629 (2017).
(6) S. Ren, R. Dawson, D. J. Adams, and A. I. Cooper, *Polym. Chem.*, **4**, 5585 (2013).
(7) B. Bonillo, R. S. Sprick and A. I. Cooper, *Chem. Mater.*, **28**, 3469 (2016).
(8) Z. Xiao, M. Zhang, W. Fan, Y. Qian, Z. Yang, B. Xu, Z. Kang, R. Wang, and D. Sun, *Chem. Eng. J.*, **326**, 640 (2017).
(9) L. Cai, Y. Li, Y. Li, H. Wang, Y. Yu, Y. Liu, and Q. Duan, *J. Hazard. Mater.*, **348**, 47 (2018).
(10) A. S. Karpov and T. J. J. Müller, *Synthesis*, **5**, 2815 (2003).
(11) Z. Li, J. He, X. Chen, Y. Cheng, and J. Yang, *Tetrahedron*, **74**, 6612 (2018).
(12) R. E. Whittaker, A. Dermenci, and G. Dong, *Synthesis*, **48**, 161 (2016).
(13) H. Deng, R. Hu, A. C. S. Leung, E. Zhao, J. W. Y. Lam, and B. Z. Tang, *Polym. Chem.*, **6**, 4436 (2015).
(14) H. Deng, Z. He, J. W. Y. Lam, and B. Z. Tang, *Polym. Chem.*, **6**, 8297 (2015).
(15) C. Zheng, H. Deng, Z. Zhao, A. Qin, R. Hu, and B. Z. Tang, *Macromolecules*, **48**, 1941 (2015).
(16) X. Tang, C. Zheng, Y. Chen, Z. Zhao, A. Qin, R. Hu, and B. Z. Tang, *Macromolecules*, **49**, 9291 (2016).
(17) J. Choi, J. H. Ko, C. W. Kang, S. M. Lee, H. J. Kim, Y. J. Ko, M. Yang, and S. U. Son, *J. Mater. Chem. A*, **6**, 6233 (2018).
(18) M. H. Kim, J. Choi, K. C. Ko, K. Cho, J. H. Park, S. M. Lee, H. J. Kim, Y. J. Ko, J. Y. Lee, and S. U. Son, *Chem. Commun.*, **54**, 5134 (2018).
(19) A. Rehman and S. J. Park, *Macromol. Res.*, **25**, 1035 (2017).
(20) D. Kim, S. Yun, S. Chun, and J. Choi, *Macromol. Res.*, **26**, 317 (2018).
(21) H. Lim, M. C. Cha, and J. Y. Chang, *Macromol. Chem. Phys.*, **213**, 1385 (2012).
(22) P. Arab, M. G. Rabbani, A. K. Sekizkardes, T. Islamoğlu, and H. M. El-Kaderi, *Chem. Mater.*, **26**, 1385 (2014).
(23) R. Dawson, E. Stöckel, J. R. Holst, D. J. Adams, and A. I. Cooper, *Energy Environ. Sci.*, **4**, 4239 (2011).
(24) J. X. Jiang, F. Su, A. Trewin, C. D. Wood, N. L. Campbell, H. Niu, C. Dickinson, A. Y. Ganin, M. J. Rosseinsky, Y. Z. Khimyak, and A. I. Cooper, *Angew. Chem. Int. Ed.*, **46**, 8574 (2007).
(25) R. J. Cox, D. J. Ritson, T. A. Dane, J. Berge, J. P. H. Charmant, and A. Kantacha, *Chem. Commun.*, 1037 (2005).
(26) S. Razzaque, C. Cai, Q. Lu, F. Huang, Y. Li, H. Tang, I. Hussain, and B. Tan, *J. Mater. Chem. B*, **5**, 742 (2017).
(27) B. Li, X. Yang, L. Xia, M. I. Majeed, and B. Tan, *Sci. Rep.*, **3**, 1 (2013).
(28) N. Kang, J. H. Park, M. Jin, N. Park, S. M. Lee, H. J. Kim, J. M. Kim, and S. U. Son, *J. Am. Chem. Soc.* **135**, 19115 (2013).
(29) Y. Lim, M. C. Cha, and J. Y. Chang, *Sci. Rep.*, **5**, 15957 (2015).
(30) Y. Chen, H. Sun, R. Yang, T. Wang, C. Pei, Z. Xiang, Z. Zhu, W. Liang, A. Li, and W. Deng, *J. Mater. Chem. A*, **3**, 87 (2015).
(31) J. Chun, J. H. Park, J. Kim, S. M. Lee, H. J. Kim, and S. U. Son, *Chem. Mater.*, **24**, 3458 (2012).
(32) J. Lee and J. Y. Chang, *RSC Adv.*, **8**, 25277 (2018).
(33) T. E. Glotova, M. Y. Dvorko, I. A. Ushakov, N. N. Chipanina, O. N. Kazheva, A. N. Chekhlov, O. A. Dyachenko, N. K. Gusarova, and B. A. Trofimov, *Tetrahedron*, **65**, 9814 (2009).

(34) W. Lu, Z. Wei, D. Yuan, J. Tian, S. Fordham, and H. C. Zhou, *Chem. Mater.*, **26**, 4589 (2014).
(35) B. Kiskan and J. Weber, *ACS Macro Lett.*, **1**, 37 (2012).
(36) S. Li, K. Han, J. Li, M. Li, and C. Lu, *Micropor. Mesopor. Mater.*, **243**, 291 (2017).
(37) P. Puthiaraj, Y. R. Lee, and W. S. Ahn, *Chem. Eng. J.*, **319**, 65 (2017).
(38) M. H. Nematollahi, A.H.S. Dehaghani, V. Pirouzfar, and E. Akhondi, *Macromol. Res.*, **24**, 782 (2016).
(39) R. Bera, S. Mondal, and N. Das, *Micropor. Mesopor. Mater.*, **257**, 253 (2018).
(40) P. Markewitz, W. Kuckshinrichs, W. Leitner, J. Linssen, P. Zapp, R. Bongartz, A. Schreiber, and T. E. Müller, *Energy Environ. Sci.*, **5**, 7281 (2012).
(41) J. Kou and L.-B. Sun, *J. Mater. Chem. A*, **4**, 17299 (2016).

